EURASIAN PHYSICAL TECHNICAL JOURNAL

2024, Volume 21, No.4 (50)

https://doi.org/10.31489/2024No4/118-130

Received: 12/04/2024 Revised: 09/09/2024 Accepted: 11/12/2024 Published online: 25/12/2024

Original Research Article

UDC: 539.192; 539.194

ANALYTICAL SOLUTION OF THE CLASS OF INVERSELY QUADRATIC YUKAWA POTENTIAL WITH APPLICATION TO QUANTUM MECHANICAL SYSTEMS

Inyang E.P.[1], Nwachukwu I. M.[1], Ekechukwu C.C.[2], Ekong I.B.[2], William E.S.[3], Lawal K.M.[1], Simon J.[1], Momoh K.O.[1], Oyelami O.A.[4]

[1] National Open University of Nigeria, Jabi-Abuja, Nigeria
[2] University of Calabar, Calabar, Nigeria
[3] Federal University of Technology, Ikot Abasi, Nigeria
[4] Open University of Nigeria, Lagos, Nigeria
*Corresponding author: einyang@noun.edu.ng

Abstract. *In our study, we applied the Exact Quantization Rule approach to tackle the radial Schrödinger equation analytically, specifically addressing the class of inversely quadratic Yukawa potential. Through this method, we successfully predicted the mass spectra of heavy mesons, including charmonium and bottomonium, across a range of quantum states by leveraging the energy eigenvalues. When compared to experimental data and other researchers' findings, our model exhibited a remarkable degree of accuracy, with a maximum error of* $0.0065\ GeV$*. We reduced our potential model to the Kratzer potential in order to further expedite our computations, and we ensured mathematical accuracy by imposing particular boundary conditions. By utilizing the acquired energy spectrum, we broadened our examination to investigate the energy spectra of homonuclear diatomic molecules, like nitrogen* (N_2) *and hydrogen* (H_2)*. One remarkable finding was that the energy spectrum reduced as the angular momentum quantum number increased in the case where the principal quantum number stayed fixed. In a similar vein, the energy spectrum consistently decreases when the angular momentum quantum number is varied. The complex interaction between the kinetic and potential energies of the electron causes this decreasing trend in the energy spectrum as the angular momentum quantum number increases in a diatomic molecule. The energy spectrum is systematically reduced as the electron's orbit lengthens and its distance from the nucleus increases, shifting the balance between these energies.*

Keywords: Schrödinger equation; Exact Quantization Rule; Homonuclear diatomic molecules; Heavy mesons; Class of Inversely Quadratic Yukawa potential

1. Introduction

Diatomic molecules are important components of the fascinating field of molecular physics. They consist of two atoms bonded together. These molecules are important because they are simple and useful for understanding molecular behavior and chemical bonding in a variety of fields such as chemistry, physics, and materials science. They are divided into two categories: homonuclear diatomic molecules, which are made up of two atoms of the same element such as oxygen (O_2), nitrogen (N_2), hydrogen (H_2), and chlorine (Cl_2), and heteronuclear diatomic molecules, which are created when two distinct elements combine. Nitric oxide (NO), hydrogen chloride (HCl), and carbon monoxide (CO) are a few examples. The electronic, vibrational, and

rotational spectra of diatomic molecules reveal important details about their composition, states of energy, and chemical properties. These molecules have recently been studied by authors [1-3]. The solution of the radial Schrödinger equation (SE) is crucial in modern physics [4], but it requires knowledge of the particular confining potential (CP) that governs a system. Quark confinements and Coulombic interactions are captured for quarkonium systems by the Cornell potential, which combines Coulomb and linear potentials [5]. The Schrödinger and semi-relativistic wave equations are usually used to solve this potential [6,7]. While the constituent quark model describes heavy mesons (HM) like charmonium and bottomonium as non-relativistic bound states of a quark-antiquark pair [8], the full description in particle physics relies on Quantum Chromodynamics (QCD) to account for the strong interaction mediating their dynamics [9]. In essence, the non-relativistic approach offers a simplified picture, whereas QCD provides a more rigorous framework. Numerous researchers have explored the Cornell potential and its variations using diverse analytical techniques [10,11]. Such as, the asymptotic iteration method (AIM) [12], Laplace transformation method [13], and others [14–17] have been proposed to solve the Schrödinger equation for such potentials. Recently, exponential-type potentials have garnered attention for studying heavy meson mass spectra [18-20]. For instance, Inyang et al. [21] investigated heavy meson mass spectra using the Yukawa potential, while Ibekwe et al. [22] examined the effect of an improved screened Kratzer potential with the mass spectra. Akpan et al. [23] presented mass spectra using a combination of the Hulthen and Hellmann potential models, and Inyang et al. [24] studied heavy meson mass spectra with the Varshni potential. Motivated by these studies, we utilize the class of inversely quadratic Yukawa potential (CIQYP) to predict heavy meson mass spectra like charmonium and bottomonium, along with the energy spectra of homonuclear diatomic molecules (HDM) such as hydrogen (H_2) and nitrogen (N_2), employing the exact quantization rule (EQR) to solve the Schrödinger equation. Furthermore, the meson is assumed to be a spinless particle for ease [26, 27]. The theory describes diatomic molecules and heavy mesons by modeling their interactions with the class of inversely quadratic Yukawa potential. It captures vibrational-rotational spectra in molecules and energy spectra in mesons, accounting for quantum effects like tunneling and binding energies. This approach bridges atomic-scale molecular behavior and quarkonium systems' fundamental particle interactions.

The class of inversely quadratic Yukawa potential is given as:

$$V(r_q) = -\frac{A_a}{r_q} - \frac{A_b}{r_q^{\,2}} + \frac{A_c e^{-\alpha r_q}}{r_q^{\,2}} \tag{1}$$

where α is the screening parameter, A_a, A_b, *and* A_c are potential strength parameters that will be determined subsequently. The potential is more appropriate compared to other potentials inspired by QCD, for example, the Cornell Potential, because it has more fitting parameters. The class of inversely quadratic Yukawa potential could find great applications in atomic physics, nuclear physics, and molecular physics. Modeling the potential to interact in the quarkonium system, Taylor series expansion is carried out in the exponential term, resulting in Eq. (2).

$$V(r_q) = \frac{\beta_{00}}{r_q^{\,2}} - \frac{\beta_{11}}{r_q} + \beta_{22} r_q^{\,2} + \beta_{33} r_q + \beta_{44}, \tag{2}$$

where

$$\beta_{00} = A_c - A_b, \beta_{11} = A_a - A_c\alpha, \beta_{22} = \frac{\alpha^4 A_c}{24}, \beta_{33} = -\frac{\alpha^3 A_c}{6}, \beta_{44} = \frac{A_c\alpha^2}{2} \tag{3}$$

2. Exact Quantization Rule formalism

This section provides a concise overview of the exact quantization rule. For a comprehensive understanding of the exact quantization rule and its implications, readers are directed to the extensive discussions available in references [28, 29].

The Schrödinger equation in one dimension is written as:

$$\frac{d^2\psi_1(\mathrm{y})}{dy^2} + \frac{2\mu_a}{\mathrm{h}^2}\left[E_{nl} - V(\mathrm{y})\right]\psi_1(\mathrm{y}) = 0 \tag{4}$$

The expression represented by Equation (4) can be alternatively formulated as follows:

$$\phi'(\mathrm{y}) + \phi(\mathrm{y})^2 + k(\mathrm{y})^2 = 0 \tag{5}$$

.

with

$$k(\mathrm{y}) = \sqrt{\frac{2\mu_a}{\mathrm{h}^2}\left[E_{nl} - V(\mathrm{y})\right]} \tag{6}$$

In the equation provided, $\phi(\mathrm{y}) = \psi_1'(\mathrm{y})/\psi_1(\mathrm{y})$ represents the logarithmic derivative of the wave function (WF), μ_a denotes the reduced mass of the quarkonium particles, $k(\mathrm{y})$ stands for momentum, and $V(\mathrm{y})$ represents a piecewise continuous real potential function of x_c. The phase angle of the SE corresponds to the logarithmic derivative $\phi(\mathrm{y})$. As indicated by Equation (6), when x increases across a node of the wave function $\psi_1(\mathrm{y})$, $\phi(\mathrm{y})$, decreases to $-\infty$, undergoes a jump to $+\infty$, and then decreases once more. We can extend the exact quantization rule to encompass the three-dimensional radial SE with spherically symmetric potential by simply substituting the variables $y \to r$ and $V(\mathrm{y}) \to V_{eff}(r)$ accordingly, as detailed in references [28, 29].

$$\int_{r_a}^{r_b} k(r_q)dr_q = N\pi + \int_{r_a}^{r_b} \phi(r_q)\left[\frac{dk(r_q)}{dr_q}\right]\left[\frac{d\phi(r_q)}{dr_q}\right]^{-1} \tag{7}$$

$$k(r_q) = \sqrt{\frac{2\mu_a}{\hbar^2}\left[E_{nl} - V_{eff}(r_q)\right]} \tag{8}$$

In this context, r_a *and* r_b refers to two turning points identified by $E = V_{eff}(r)$. $N = n+1$, which represents the number of nodes $\phi(r)$ within the region $E_{nl} = V_{eff}(r)$ is incremented by 1 compared to the count of nodes in the wave function $\psi_1(r_q)$. The expression can be decomposed into two terms: $N\pi$, originating from the nodes of the logarithmic derivatives of the wave function, and a second term known as the quantum correction. Notably, the quantum correction, denoted as (Q_c), primarily concerns the ground state, simplifying the calculation process. i.e.,

$$Q_c = \int_{r_a}^{r_b} k_0'(r_q)\frac{\phi_0}{\phi_0'}dr_q \tag{9}$$

3. Analytical solutions of the Schrödinger equation with the class of inversely quadratic Yukawa potential

The Schrödinger equation is given by [30].

$$\frac{d^2R(r_q)}{dr_q^2} + \frac{2\mu_a}{\mathrm{h}^2}\left[E_{nl} - V(r_q) - \frac{l(l+1)\mathrm{h}^2}{2\mu_a r_q^2}\right]R(r_q) = 0 \tag{10}$$

In this equation, l, corresponds to the angular momentum, μ_a, is the reduced mass, r_q represents the distance between the interacting particles, and $\hbar$ denotes the reduced Planck constant.

By substituting Equation (2) into Equation (10), we derive

$$\frac{d^2R(r_q)}{dr_q^2} + \frac{2\mu_a}{\mathrm{h}^2}\left[E_{nl} - V_{eff}(r_q)\right]R(r_q) = 0 \tag{11}$$

where

$$V_{eff}(r_q) = \frac{\beta_{00}}{r_q^2} - \frac{\beta_{11}}{r_q} + \beta_{22}r_q^2 + \beta_{33}r_q + \beta_{44} + \frac{l(l+1)\mathrm{h}^2}{2\mu_a r_q^2} \tag{12}$$

Transformation of the coordinate of Eq. (11) from r_q to s is given below;

$$s = \frac{1}{r_q} \tag{13}$$

After substituting Equation (13) into Equation (12), we obtain Equation (14).

$$V_{eff}(\mathrm{s}) = \beta_{00}s^2 - \beta_{11}s + \frac{\beta_{22}}{s^2} + \frac{\beta_{33}}{s} + \beta_{44} + \frac{l(l+1)\mathrm{h}^2 s^2}{2\mu_a} \tag{14}$$

To simplify the analysis of the third and fourth terms in equation (14), we introduce an approximation strategy. This strategy involves assuming a characteristic radius, r_0, for the meson. We will then proceed by expanding $\frac{\beta_{33}}{s}$ and $\frac{\beta_{22}}{s^2}$ in a power series around r_0; i.e. around $\delta \equiv \frac{1}{r_0}$, up to the second order. This is similar to the Pekeris-type approximation which helps to deform the centrifugal term [31].

Setting $z_c = s - \delta$ and around $z_c = 0$ it can be expanded as

$$\frac{\beta_{33}}{s} = \frac{\beta_{33}}{z_c + \delta} = \frac{\beta_{33}}{\delta\left(1 + \frac{z_c}{\delta}\right)} = \frac{\beta_{33}}{\delta}\left(1 + \frac{z_c}{\delta}\right)^{-1} \tag{15}$$

which yields

$$\frac{\beta_{33}}{s} = \beta_{33}\left(\frac{3}{\delta} - \frac{3s}{\delta^2} + \frac{s^2}{\delta^3}\right) \tag{16}$$

Similarly,

$$\frac{\beta_{22}}{s^2} = \beta_{22}\left(\frac{6}{\delta^2} - \frac{8s}{\delta^3} + \frac{3s^2}{\delta^4}\right) \tag{17}$$

The next step involves utilizing equations (16) and (17) within equation (14). This substitution leads to

$$V_{eff}(\mathrm{s}) = \xi_{11} + \xi_{22}s + \xi_{33}s^2 \tag{18}$$

where

$$\left.\begin{aligned} \xi_{11} &= \frac{6\beta_{22}}{\delta^2} + \frac{3\beta_{33}}{\delta} + \beta_{44}, \quad \xi_{22} = -\beta_{11} - \frac{3\beta_{33}}{\delta^2} - \frac{8\beta_{22}}{\delta^3} \\ \xi_{33} &= \frac{3\beta_{33}}{\delta^4} + \frac{\beta_{33}}{\delta^3} + \beta_{00} + \frac{l(l+1)\mathrm{h}^2}{2\mu_a} \end{aligned}\right\} \tag{19}$$

We can express the non-linear Riccati equation describing the ground state using a new variable, denoted by s as**,**

$$-s^2\phi'(\mathrm{s}) + \phi^2(\mathrm{s}) = k(\mathrm{s}), \tag{20}$$

where

$$k(\mathrm{s}) = \sqrt{\frac{2\mu_a}{\mathrm{h}^2}\left[\xi_{33}s^2 + \xi_{22}s + \xi_{11} - E\right]} \tag{21}$$

The quantization rule comes into play as we analyze the potential. The first step involves calculating the turning points, labeled s_a and s_b. We achieve this by solving the equation within the square brackets of Eq. (21).

$$\left.\begin{aligned} s_a &= \frac{-\xi_{22} - \sqrt{\xi_{22}^{\ 2} - 4\xi_{33}(\xi_{11} - E)}}{2\xi_{33}} \\ s_b &= \frac{-\xi_{22} + \sqrt{\xi_{22}^{\ 2} - 4\xi_{33}(\xi_{11} - E)}}{2\xi_{33}} \end{aligned}\right\} \tag{22}$$

From Eq. (22) we get,

.

$$\left.\begin{aligned} s_a s_b &= \frac{\xi_{11}-E}{\xi_{33}} \\ s_a + s_b &= -\frac{\xi_{22}}{\xi_{33}} \end{aligned}\right\} \tag{23}$$

Also, from Eq. (21) we have

$$k(\mathrm{s}) = \sqrt{\frac{2\mu_a}{\mathrm{h}^2}\xi_{33}\left(x_c{}^2 + \frac{\xi_{22}}{\xi_{33}}x + \frac{\xi_{11}-E}{\xi_{33}}\right)} \tag{24}$$

Substituting Eq. (23) into Eq. (24) gives

$$k(\mathrm{s}) = \sqrt{\frac{2\mu_a\xi_{33}}{\mathrm{h}^2}(s-s_a)(s-s_b)} \tag{25}$$

where $k(\mathrm{s})$ is the momentum between the two turning points s_a and s_b.

Because the logarithmic derivative possesses only one zero and lacks poles for the ground state, we propose a trial solution for the ground state wave function

$$\phi_0(\mathrm{s}) = A_1 + B_2 s \tag{26}$$

We can solve for the ground state energy by incorporating Eq. (26) into Eq. (20). This involves solving the resulting non-linear Riccati equation, which yields

$$E_0 = \xi_{11} - \frac{\mathrm{h}^2 A_1^2}{2\mu_a} \tag{27}$$

Also, A_1 and B_2 are obtained as follows

$$\left.\begin{aligned} A_1 &= \frac{\mu_a\xi_{22}}{B_2\mathrm{h}^2} \\ B_2 &= \frac{1}{2} + \sqrt{\frac{1}{4} - \frac{2\mu_a\xi_{33}}{\mathrm{h}^2}} \end{aligned}\right\} \tag{28}$$

The positive sign is chosen for the square root of B_2. This selection is crucial because it ensures that the logarithmic derivatives $\phi_0(\mathrm{s})$ behave as needed, specifically by decaying exponentially. Having established this, we can now determine the quantum correction, which is

$$\int_{r_a}^{r_b}\phi(r_q)\left[\frac{dk(r_q)}{dr_q}\right]\left[\frac{d\phi(r_q)}{dr_q}\right]^{-1}dr_q = -\int_{s_a}^{s_b}\frac{k_0'(\mathrm{s})}{s^2}\frac{\phi_0(\mathrm{s})}{\phi_0'(\mathrm{s})}ds \tag{29}$$

From Eq. (29) we have

$$= \sqrt{\frac{2\mu_a\xi_{33}}{\mathrm{h}^2}}\int_{s_a}^{s_b}\left(\frac{\frac{A_1}{B_2} - \frac{s_a+s_b}{2}}{s\sqrt{(s-s_a)(s-s_b)}} + \frac{\frac{A_1}{B_2}\left(\frac{s_a+s_b}{2}\right)}{s^2\sqrt{(s-s_a)(s-s_b)}}\right)ds \tag{29a}$$

By referring to the integrals in Appendix A, we achieved the following

$$= \pi\sqrt{\frac{2\mu_a\xi_{33}}{\mathrm{h}^2}}\left[\frac{\frac{A_1}{B_2} - \frac{s_a+s_b}{2}}{\sqrt{1+(s_a+s_b)+s_a s_b}} + \frac{\frac{A_1}{B_2}\left(\frac{s_a+s_b}{2}\right)\left(\sqrt{s_a s_b} - \frac{1}{2(s_a+s_b)}\right)}{\sqrt{s_a s_b}}\right] \tag{29b}$$

We substitute Eq. (23) into Eq.(29b) and obtain

$$= \pi\sqrt{\frac{2\mu_a\xi_{33}}{\mathrm{h}^2}}\left[\frac{\frac{A_1}{B_2}+\frac{\xi_{22}}{2\xi_{33}}}{\sqrt{\frac{\mathrm{h}^2}{2\mu\xi_3}}\left(A_1+B_2\right)}-\frac{\frac{A_1\xi_{22}}{2B_2\xi_{33}}\left(\sqrt{\frac{\mathrm{h}^2}{2\mu_a\xi_{33}}}A_1+\frac{\xi_{33}}{2\xi_{22}}\right)}{\sqrt{\frac{\mathrm{h}^2}{2\mu_a\xi_{33}}}A_1}\right] \tag{29c}$$

Inserting Eq. (29c) into Eq. (7), Eq.(29d) is gotten as;

$$= \pi\sqrt{\frac{2\mu_a\xi_{33}}{\mathrm{h}^2}}\left[\frac{\frac{A_1}{B_2}+\frac{\xi_{22}}{2\xi_{33}}}{\sqrt{\frac{\mathrm{h}^2}{2\mu_a\xi_{33}}}\left(A_1+B_2\right)}-\frac{\frac{A_1\xi_{22}}{2B_2\xi_{33}}\left(\sqrt{\frac{\mathrm{h}^2}{2\mu_a\xi_{33}}}A_1+\frac{\xi_{33}}{2\xi_{22}}\right)}{\sqrt{\frac{\mathrm{h}^2}{2\mu_a\xi_{33}}}A_1}\right]+N\pi \tag{29d}$$

Furthermore, the integral of Eq.(9) is obtain as

$$\int_{r_a}^{r_b}k(r_q)dr_q=-\int_{s_a}^{s_b}\frac{k(\mathrm{s})}{s^2}ds \tag{30}$$

From Eq.(30) we have

$$=-\sqrt{\frac{2\mu_a\xi_{33}}{\mathrm{h}^2}}\int_{s_a}^{s_b}\frac{\sqrt{\left(s-s_a\right)\left(s-s_b\right)}}{s^2}ds \tag{30a}$$

After utilizing Eq. (31), Eq. (30a) takes the following form

$$=-\sqrt{\frac{2\mu_a\xi_{33}}{\mathrm{h}^2}}\left[\frac{\left(s_a+s_b\right)-\sqrt{s_as_b}}{2\sqrt{s_as_b}}\right] \tag{30b}$$

Incorporating Eq. (23) into Eq. (30b), we get

$$-\sqrt{\frac{2\mu_a\xi_{33}}{\mathrm{h}^2}}\left[\frac{-\frac{\xi_{22}}{\xi_{33}}-\sqrt{\frac{\xi_{11}-E}{\xi_{33}}}}{2\sqrt{\frac{\xi_{11}-E}{\xi_{33}}}}\right] \tag{30c}$$

Since Eq. (27a) lacked a solution in standard integral tables, we employed Maple software to evaluate it. This resulted in the following valuable integral:

$$\int_a^b\frac{\sqrt{\left(s-a\right)\left(b-s\right)}}{s^2}ds=\frac{\left(a+b\right)-\sqrt{ab}\pi_a}{2\sqrt{ab}} \tag{31}$$

The energy equation governing the CIQYP is obtained by equating Eqs. (29d) and (30c). We achieve this after incorporating Eqs. (19), (28), and (3).

$$E_{nl}=\frac{\alpha^4A_c}{4\delta^2\mathrm{h}^2}-\frac{\alpha^3A_c}{2\delta\mathrm{h}^2}-\frac{\frac{\mu_a}{2\mathrm{h}^2}\left(\frac{\alpha^4A_c^2}{3\delta^3}-\frac{\alpha^3A_c}{2\delta^2}+A_c\alpha^2+A_a^2-A_c\alpha\right)}{\left[n+\frac{1}{2}+\sqrt{\frac{4\mu_a\alpha^3A_c}{3\delta^3\mathrm{h}^2}+\left(l+\frac{1}{2}\right)^2+\frac{2\mu_a(A_c-A_b)}{\mathrm{h}^2}+\frac{\mu_a\alpha^2A_c}{\delta^4\mathrm{h}^2}}\right]^2} \tag{32}$$

4. Application to Diatomic Molecules

Diatomic molecules, which are made up of just two atoms bonded together are the basic building blocks of physics and chemistry. These combinations are essential to everything in our world, including the materials we use and the air we breathe. By setting $A_a=2D_er_e, A_b=-D_er_e^2, A_c=0$ of Eq.(1), we have the Kratzer potential [32] and the energy equation is given as Eq.(33),

$$E_{nl} = -\frac{2\mu_a}{\hbar^2} D_e^2 r_e^2 \left[n + \frac{1}{2} + \sqrt{\left(l + \frac{1}{2} \right)^2 + \frac{2\mu_a D_e r_e^2}{\hbar^2}} \right]^{-2} \tag{33}$$

5. Application to Heavy Mesons

Based on the theoretical framework provided in references [33, 34], we compute the mass spectra for heavy meson

$$M_x = 2m_w + E_{nl} \tag{34}$$

where m_w is quarkonium mass and E_{nl} is energy eigenvalues.

The mass spectra of the class of inversely quadratic Yukawa potential for heavy mesons can be derived by incorporating Eq. (32) into Eq. (34).

$$M_x = 2m_w + \frac{\alpha^4 A_c}{4\delta^2 \hbar^2} - \frac{\alpha^3 A_c}{2\delta \hbar^2} - \frac{\frac{\mu_a}{2\hbar^2}\left(\frac{\alpha^4 A_c^2}{3\delta^3} - \frac{\alpha^3 A_c}{2\delta^2} + A_c\alpha^2 + A_a^2 - A_c\alpha \right)}{\left[n + \frac{1}{2} + \sqrt{\frac{4\mu_a \alpha^3 A_c}{3\delta^3 \hbar^2} + \left(l + \frac{1}{2} \right)^2 + \frac{2\mu_a (A_c - A_b)}{\hbar^2} + \frac{\mu_a \alpha^2 A_c}{\delta^4 \hbar^2}} \right]^2} \tag{35}$$

In this work, we rely on the Chi-square function [24] to determine how closely our numerical predictions match the actual values.

$$\chi^2 = \frac{1}{k_a} \sum_{j=1}^{k_a} \frac{\left(M_j^{\text{Exp.}} - M_j^{Theo.} \right)}{\nabla_j} \tag{36}$$

where k_a represent number of mesons sample, $M_j^{\text{Exp.}}$ is the experimental value of mesons, while $M_j^{Theo.}$ is the corresponding theoretical prediction. The ∇_j quantity is the experimental uncertainty of the masses. Intuitively, $\nabla_j = 1$.

6. Discussion of results

The analytical calculations agree with experiments involving diatomic molecular spectroscopy, where potential energy curves match spectroscopic constants. They align with data on vibrational-rotational spectra, energy levels in quantum dots, and heavy quarkonium mass spectra, validating models in plasma and condensed matter systems under the class of inversely quadratic Yukawa interactions.

Our predictions for the mass spectra of heavy mesons in various quantum states are summarized in Tables 1 and 2. To achieve these predictions, we first needed to determine the free parameters in equation (35). This was accomplished by solving a system of two algebraic equations. The specific values used for bottomonium and charmonium systems, as referenced in [35], are $m_b = 4.823\,GeV$, and $m_c = 1.209\,GeV$, respectively. The experimental data is taken from [36, 37]. The predicted mass spectra for charmonium and bottomonium, shown in Tables 1 and 2, exhibit excellent agreement with experimental data. This represents a significant improvement compared to earlier works like Refs. [12, 13]. This simply implies that one approach to understanding the behavior of quark-antiquark pairs in mesons is to use potential models. These models describe the interaction between quarks and antiquarks as an effective potential energy. The potential energy includes contributions from the strong force as well as other forces. Our predictions agree with experimental data within a maximum margin of error of $0.0065\,GeV$. Our potential model was simplified to the Kratzer potential through the application of specific boundary conditions, ensuring the mathematical precision of our analytical calculations. Additionally, we utilized the energy spectrum outlined in Eq. (33) to examine the energy spectra of HDM such as hydrogen (H_2) and nitrogen (N_2). The spectroscopic data for these molecules, sourced from references [38], are presented in Table 3. The calculations were carried out utilizing the conversions outlined by 1 amu = 931.494028 MeV/c^2 and $\hbar c = 1973.29$ eV Å [1-3].

The selection of these diatomic molecules was based on extensive applications and studies conducted by various researchers. Tables 4 and 5 present the numerical energy eigenvalues for the chosen homonuclear diatomic molecules across different quantum numbers n and l. Notably, for a fixed principal quantum number

n, the energy spectrum decreases with an increase in angular momentum quantum l. Similarly, maintaining the angular momentum quantum l constant while varying the principal quantum number n yields the same observed trend. This suggests that the behavior of the angular momentum and its impact on the energy levels, specifically, are the fundamental principles of quantum mechanics and explain the decrease in the energy spectrum with increasing angular momentum quantum number for a fixed principal quantum number in a HDM. An electron orbiting a nucleus in a diatomic molecule, for example, has quantized angular momentum in quantum mechanics, which means it can only take on specific discrete values determined by the quantum numbers n and l. Both the angular momentum quantum number and the principal quantum number of an electron in an atom or molecule define its energy. The electron's orbit grows more elliptical and farther from the nucleus as the angular momentum quantum number rises while the principal quantum number remains constant. The electron's potential energy decreases with increasing distance, resulting in lower energy levels or, to put it another way, a reduction in the energy spectrum. These findings align well with results previously obtained using diverse analytical and numerical methods [39, 40].

Table 1. Mass spectra of charmonium in (GeV) (m_c =1.209 GeV, μ_a = 0.6045 GeV, $A_a = -19252.67309\ GeV$, $A_b = -1.94850856910^6\ GeV$, $A_c = -1.9497828810^6 GeV$, $\alpha = 0.01\ GeV$, $\delta = 0.371\ GeV$)

State	Present work	AIM [12]	LTM [13]	Experiment [36,37]
1s	3.09588	3.096	3.0963	3.096
2s	3.68568	3.686	3.5681	3.686
1p	3.52447	3.214	3.5687	3.525
2p	3.77234	3.773	3.5687	3.773
3s	4.04010	4.275	4.0400	4.040
4s	4.26322	4.865	4.5119	4.263
1d	3.77110	3.412	4.0407	3.770
2d	4.15909	-	-	4.159

Table 2. Mass spectra of bottomonium in (GeV) (m_b = 4.823 GeV, μ_a = 2.4115 GeV, $A_a = -11852.70018\ GeV$, $A_b = -1.19335194110^6\ GeV$, $A_c = -1.19413808310^6\ GeV$, $\alpha = 0.01\ GeV$, $\delta = 0.371\ GeV$).

State	Present work	AIM [12]	LTM [13]	Experiment [36,37]
1s	9.46023	9.460	9.745	9.460
2s	10.02345	10.023	10.023	10.023
1p	9.89923	9.492	10.025	9.899
2p	10.26098	10.038	10.303	10.260
3s	10.35587	10.585	10.302	10.355
4s	10.58076	11.148	10.580	10.580
1d	10.16467	9.551	10.303	10.164

Table 3. Spectroscopic parameters of the selected HDM [38]

Molecules	$D_e(eV)$	$r_e\left(\overset{g}{A}\right)$	$\mu_a(MeV)$
H_2	4.7446000000	0.7416	0.05021684305
N_2	11.938190000	1.0940	0.65235787010

In addition, Fig. 1 is the variation of energy spectra against the angular quantum number, which shows an asymptotic convergence of the energy. Understanding the stability of diatomic molecules requires an understanding of the asymptotic convergence of energy, which occurs when the internuclear separation approaches a certain value as it grows very large. When they approach each other, electron sharing attracts them together and creates a stable bound state with a minimum energy configuration. The most precise framework for characterizing the energy states of diatomic molecules is provided by quantum mechanics.

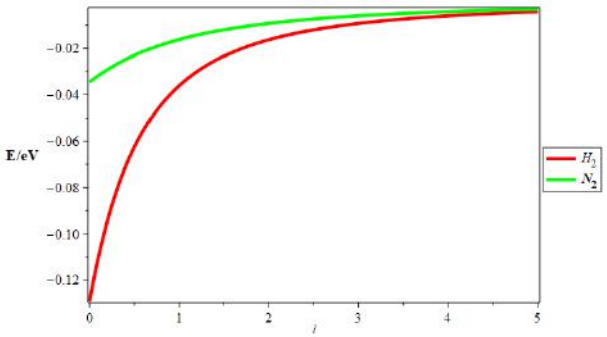

Fig.1. The correlation between the angular momentum quantum number (ℓ) and the variation in energy levels for the homonuclear diatomic molecules.

Table 4. Energy spectra (in eV) for the various *n* and *l* quantum numbers for a HDM at constant n

n	*l*	N_2	H_2
0	0	−11.88375321672634	−4.565204473204863
	1	−11.883257920816611	−4.551938675793838
	2	−11.882267452916444	−4.525638129919935
	3	−11.88078206078689	−4.4867549364956085
1	0	−11.776112900792786	−4.238616688471602
	1	−11.775624318967708	−4.226747699496392
	2	−11.774647277141154	−4.203210857813765
	3	−11.773182018884329	−4.168399926608872
	4	−11.771228909364144	−4.122884944668811
2	0	−11.669928460893514	−3.945860680848302
	1	−11.669446472347172	−3.9351990851508365
	2	−11.668482615027564	−3.914051903440431
	3	−11.667037128406324	−3.882763865567736
	4	−11.665110371504726	−3.8418344039298025
	5	−11.662702822670521	−3.7918979616955264
3	0	−11.565173759877975	−3.6824199205172485
	1	−11.564698246509348	−3.6728073518278963
	2	−11.563747337538615	−3.653736983693575
	3	−11.562321268425762	−3.625512072868766
	4	−11.560420392178223	−3.588572275743318
	5	−11.558045179132064	−3.5434766480219393
	6	−11.555196216660608	−3.490882938850404

Table 5. Energy spectra (in eV) for the various *n* and *l* quantum numbers for a HDM at constant *l*

l	n	N_2	H_2
0	0	−11.88375321672634	−4.565204473204863
	1	−11.776112900792786	−4.238616688471602
	2	−11.669928460893514	−3.945860680848302
	3	−11.565173759877975	−3.6824199205172485
1	0	−11.883257920816611	−4.551938675793838
	1	−11.775624318967708	−4.226747699496392
	2	−11.669446472347172	−3.9351990851508365
	3	−11.564698246509348	−3.6728073518278963
	4	−11.4613540908605	−3.4358103946306726
2	0	−11.882267452916444	−4.525638129919935
	1	−11.774647277141154	−4.203210857813765
	2	−11.668482615027564	−3.914051903440431
	3	−11.563747337538615	−3.653736983693575
	4	−11.460415899344495	−3.418553558957142
	5	−11.358463323244653	−3.2053677272267476
3	0	−11.88078206078689	−4.4867549364956085
	1	−11.773182018884329	−4.168399926608872
	2	−11.667037128406324	−3.882763865567736
	3	−11.562321268425762	−3.625512072868766
	4	−11.45900890150587	−3.3930046311567494
	5	−11.357075058128967	−3.182166919054122
	6	−11.256495321607867	−2.990387440908319

7. Conclusion

Our investigation utilized the exact quantization rule approach to obtain the approximate solutions of the Schrödinger equation for energy eigenvalues using a recently proposed potential known as the class of inversely quadratic Yukawa potential. Using the current findings, we calculated the heavy-meson masses (charmonium and bottomonium) for various quantum states. We observe that the mass spectra of the mesons acquired in this work are consistent with findings from other investigations and the experimental measurements. This simply implies that one approach to understanding the behavior of quark-antiquark pairs in mesons is to use potential models. These models describe the interaction between quarks and antiquarks as an effective potential energy. The potential energy includes contributions from the strong force as well as other forces. Also, our potential model was simplified to the Kratzer potential through the application of specific boundary conditions, ensuring the mathematical precision of our analytical calculations.

We utilized the energy spectrum to examine the energy spectra of homonuclear diatomic molecules such as hydrogen (H_2) and nitrogen (N_2). Notably, for a fixed principal quantum number n, the energy spectrum decreases with an increase in angular momentum quantum l. Similarly, maintaining the angular momentum quantum number l constant while varying the principal quantum number n yields the same observed trend. This implies that the decrease in the energy spectrum with increasing angular momentum quantum number for a fixed principal quantum number in a diatomic molecule arises from the interplay between the electron's kinetic and potential energies as its orbit becomes more elongated and its distance from the nucleus increases. The analytical solution notably differs by incorporating quantum mechanical principles, capturing discrete energy spectra and wavefunction behaviors that are absent in classical solutions. It accounts for state quantization, and potential-specific features, enabling precise predictions in microscopic systems—unlike classical approaches, which treat energy as continuous and overlook quantum phenomena.

Conflict of interest statement

The authors declare that they have no conflict of interest in relation to this research, whether financial, personal, authorship or otherwise, that could affect the research and its results presented in this paper.

CRediT author statement

Inyang E.P.: Conceptualization, Methodology, Writing-Original draft preparation, Funding acquisition; **Nwachukwu I. M.:** Software Funding acquisition; **William E.S:** Data curation; **Ekechukwu C.C.**: Visualization; **Ekong I.B.**: Investigation; **Lawal K. M.:** Validation, Funding acquisition; **Simon J., Momoh K O., Oyelami O.A.:** Writing- Reviewing and Editing. The final manuscript was read and approved by all authors.

Funding

This research was supported by the 2024 Senate Research Grant from the National Open University of Nigeria: with grant number NOUN/DRA/SRG/AW/045.

Acknowledgements

Inyang, E.P., Nwachukwu, I.M., and Lawal, K.M. gratefully acknowledge the National Open University of Nigeria for the 2024 Senate Research Grant award. The authors also thank the reviewers for valuable suggestions that have significantly enhanced the quality of the manuscript

References

1 Inyang E.P., Ayedun F., Ibanga E.A., Lawal K.M., Okon I. B., William E.S., Ekwevugbe O., Onate C.A., Antia A. D., Obisung E. O. (2022) Analytical Solutions of the N-Dimensional Schrödinger equation with modified screened Kratzer plus Inversely Quadratic Yukawa potential and Thermodynamic Properties of selected Diatomic Molecules. *Results in Physics*, 43, 106075. DOI:10.1016/j.rinp.2022.106075.

2 Inyang E.P., Ali N., Endut R., Aljunid S.A. (2024) Energy Spectra, Expectation Values, and Thermodynamic Properties of HCl And LiH Diatomic Molecules. *Eurasian Physical Technical Journal*, 21, 1(47), 124 – 137. DOI:10.31489/2024No1/124-137.

3 Inyang E.P., Ntibi J.E., Obisung E.O., William E.S., Ibekwe E.E., Akpan I.O., Inyang E.P. (2022) Expectation Values and Energy Spectra of the Varshni Potential in Arbitrary Dimensions. *Jordan Journal of Physics*, 5, 495 – 509. DOI: 10.47011/15.5.7.

4 Kumar R., Chand F. (2013) Asymptotic study to the N-dimensional radial Schrödinger equation for the quark-antiquark system. *Communications in Theoretical Physics*, 59(5), 528. DOI: 10.1088/0253-6102/59/5/02.

.

5 Mutuk H. (2018) Mass Spectra and Decay constants of Heavy-light Mesons: A case study of QCD sum Rules and Quark model. *Advances in High Energy Physics*, *2018*. DOI: 10.1155/2018/8095653.

6 William E.S., Inyang S.O., Ekerenam O.O., Inyang E.P., Okon I.B., Okorie U.S., Ita B.I., Akpan I.O., Ikot A.N. (2024) Theoretic analysis of non-relativistic equation with the Varshni-Eckart potential model in cosmic string topological defects geometry and external fields for the selected diatomic molecules. *Molecular Physics*, *122*(3), e2249140. DOI: 10.1080/00268976.2023.2249140.

7 Hassanabadi S., Rajabi A.A., Zarrinkamar S. (2012) Cornell and kratzer potentials within the semirelativistic treatment. *Modern Physics Letters A*, *27*(10), 1250057. DOI: 10.1142/S0217732312500575.

8 Vega A., Flores J. (2016) Heavy quarkonium properties from Cornell potential using variational method and supersymmetric quantum mechanics. *Pramana*, *87*, 1-7. DOI: 10.1007/s12043-016-1278-7.

9 Ciftci H., Kisoglu H.F. (2018) Nonrelativistic-Arbitrary l-states of quarkonium through Asymptotic Iteration method. Advances in High Energy Physics, 4549705. DOI: 10.1155/2018/4549705.

10 Carrington M.E., Czajka A., Mrówczyński S. (2020) Heavy quarks embedded in glasma. *Nuclear Physics A*, *1001*, 121914. DOI: 10.1016/j.nuclphysa.2020.121914.

11 Allosh M., Mustafa Y., Khalifa Ahmed N., Sayed Mustafa A. (2021) Ground and Excited state mass spectra and properties of heavy-light mesons. *Few-Body Systems*, *62*(2), 26. DOI: 10.1007/s00601-021-01608-1.

12 Rani R., Bhardwaj S.B., Chand F. (2018) Mass spectra of heavy and light mesons using asymptotic iteration method. *Communications in Theoretical Physics*, *70*(2), 179. DOI: 10.1088/0253-6102/70/2/179.

13 Abu-Shady M., Khokha E.M. (2018) Heavy-light mesons in the nonrelativistic quark model using laplace transformation method. *Advances in high energy physics*, *2018*. DOI: 10.1155/2018/7032041.

14 Abu-Shady M., Inyang, E.P. (2022) Heavy-meson masses in the framework of trigonometric Rosen-Morse potential using the generalized fractional Derivative. *arXiv preprint arXiv:2209.00566*. DOI: 10.26565/2312-4334-2022-4-06.

15 Inyang E.P., Obisung E.O., Amajama J., Bassey D.E., William E.S., Okon I.B. (2022) The Effect of Topological Defect on The Mass Spectra of Heavy and Heavy-Light Quarkonia. *Eurasian Physical Technical Journal*, 9, 4(42), 78 – 87. DOI: 10.31489/2022No4/78-87.

16 Ikot A.N., Obagboye L.F., Okorie U.S., Inyang E.P., Amadi P.O., Abdel-Aty A. (2022) Solutions of Schrodinger equation with generalized Cornell potential (GCP) and its applications to diatomic molecular systems in D-dimensions using Extended Nikiforov–Uvarov (ENU) formalism. *The European Physical Journal Plus*, 137, 1370 DOI:10.1140/epjp/s13360-022-03590-x.

17 Omugbe E., Eyube E.S., Onate C.A., Njoku *I*.J., Jahanshir A., Inyang E.P., Emeje K.O. (2024) Nonrelativistic energy equations for diatomic molecules constrained in a deformed hyperbolic potential function. *Journal of Molecular Modeling*, *30*(3), 1-10. DOI: 10.1007/s00894-024-05855-x.

18 Purohit K.R., Jakhad P., Rai A.K. (2022) Quarkonium spectroscopy of the linear plus modified Yukawa potential. *Physica Scripta*, *97*(4), 044002. DOI: 10.1088/1402-4896/ac5bc2.

19 Purohit K.R., Rai A.K., Parmar R.H. (2023) Spectroscopy of heavy-light mesons (cs^{-}, cq^{-}, bs^{-}, bq^{-}) for the linear plus modified Yukawa potential using Nikiforov–Uvarov method. *Indian Journal of Physics*, 1-13. DOI:10.1007/s12648-023-02852-3.

20 Inyang E.P., Inyang E.P., Akpan I.O., Ntibi J.E., William E.S. (2021) Masses and thermodynamic properties of a Quarkonium system. *Canadian Journal Physics*, 99, 982 – 990. DOI: 10.1139/cjp-2020-0578.

21 Inyang E.P., Inyang E.P., Ntibi J. E., Ibekwe E. E., William E. S. (2021) Approximate solutions of D-dimensional Klein-Gordon equation with Yukawa potential via Nikiforov-Uvarov method. *Indian Journal of Physics*, 95, 2733 - 2739. DOI: 10.1007/s12648-020-01933-x.

22 Ibekwe E.E., Okorie U.S., Emah J.B., Inyang E.P., Ekong S.A. (2021) Mass spectrum of heavy quarkonium for screened Kratzer potential (SKP) using series expansion method. *European Physical Journal Plus*, 87, 1- 11. DOI:10.1140/epjp/s13360-021-01090-y.

23 Akpan I.O., Inyang E.P., William E.S. (2021) Approximate solutions of the Schrödinger equation with Hulthen-Hellmann Potentials for a Quarkonium system. *Revista mexicana de fisica*, 67(3), 482-490. DOI:10.31349/revmexfis.67.482.

24 Inyang E.P., Inyang E.P., William E.S. (2021). Study on the applicability of Varshni potential to predict the mass-spectra of the Quark-Antiquark systems in a non-relativistic framework. *Jordan Journal of Physics*, *14*(4), 339-347. DOI: 10.47011/14.4.8.

25 Patrick I.E., Joseph N., Akpan I.E., Funmilayo A., Peter I.E., Sunday W.E. (2023). Thermal properties, mass spectra and root mean square radii of heavy quarkonium system with class of inversely quadratic Yukawa potential. *In AIP Conference Proceedings*, AIP Publishing, 2679, 1. DOI: 10.1063/5.0112829.

26 Grinstein B. (2000) A modern introduction to quarkonium theory. *International Journal of Modern Physics A*, 15(04), 461-495. DOI: 10.1142/S0217751X00000227.

27 Lucha W., Schöberl F. F., Gromes D. (1991). Bound states of quarks. *Physics reports*, *200*(4), 127-240. DOI:10.1016/0370-1573(91)90001-3.

28 Ma Z.Q., Xu B.W. (2005) Quantum correction in exact quantization rules. *Europhysics Letters*, 69(5), 685. DOI: 10.1209/epl/i2004-10418-8.

29 Ma Z.Q., Xu B.W. (2005) Exact quantization rules for bound states of the Schrödinger equation. *International Journal of Modern Physics E*, 14(04), 599-610. DOI: 10.1142/S0218301305003429.

30 William E.S., Inyang E.P., Thompson E.A. (2020) Arbitrary -solutions of the Schrödinger equation interacting with Hulthén-Hellmann potential model. *Revista Mexicana Fisica*, 66, 730 - 741. DOI: 10.31349/RevMex Fis.66.730.

31 Abu-Shady M., Edet C.O., Ikot A.N. (2021) Non-relativistic quark model under external magnetic and Aharanov–Bohm (AB) fields in the presence of temperature-dependent confined Cornell potential. *Canadian Journal of Physics*, 99(11), 1024-1031. DOI: 10.11139/cjp-2020-0101.

32 Bayrak O., Boztosun I., Ciftci H. (2007) Exact analytical solutions to the Kratzer potential by the asymptotic iteration method. *International Journal of Quantum Chemistry*, 107(3), 540-544. DOI: 10.1002/qua.21141.

33 Omugbe E., Osafile O.E., Okon I.B., Inyang E.P., William E.S., Jahanshir A. (2022) Any L-state energy of the spinless Salpeter equation under the Cornell potential by the WKB Approximation method: An Application to mass spectra of mesons. *Few-Body Systems*, 63, 1-7. DOI: 10.1007/s00601-021-01705-1.

34 Inyang E.P., Ali N., Endut R., Rusli N., Aljunid S.A., Ali N.R., Asjad M.M. (2024) Thermal Properties and Mass Spectra of Heavy Mesons in the Presence of a Point-Like Defect. *East European Journal of Physics*, (1), 156-166. DOI: 10.26565/2312-4334-2024-1-13.

35 Olive R., Groom D. E., Trippe T.G. (2014) Particle Data Group, *Chinese Physics C.*, 38, 60. DOI: 10.1088/1674-1137/38/9/090001.

36 Barnett R.M., Carone C.D., Groom D.E., Trippe T.G., Wohl C.G. Particle Data Group. *Physical Review D.*, 92,656. DOI: 10.1103/PhysRevD.54.1.

37 Tanabashi M., Carone, C. D., Trippe T.G., Wohl C.G. (2018) Particle Data Group. *Physical Review D.*, 98, 546. DOI:10.1103/PhysRevD.98.030001.

38 Inyang E.P., William E.S., Ntibi J.E., Obu J.A., Iwuji P.C., Inyang E.P. (2022) Approximate solutions of the Schrödinger equation with Hulthén plus screened Kratzer Potential using the Nikiforov–Uvarov–functional analysis (NUFA) method: an application to diatomic molecules. *Canadian Journal of Physics*, 100(10), 463-473. DOI:10.1139/cjp-2022-0030.

39 Flügge S. (2012) *Practical quantum mechanics*. Springer Science & Business Media. DOI:10.1007/978-3-642-6199.

40 Vigo-Aguiar J., Simos T.E. (2005) Review of multistep methods for the numerical solution of the radial Schrödinger equation. *International journal of quantum chemistry*, 103(3), 278-290. DOI: 10.1002/qua.20495.

AUTHORS' INFORMATION

Inyang, Etido Patrick – Dr. (Sci.), Department of Physics, Faculty of Science, National Open University of Nigeria, Abuja, Nigeria; https://orcid.org/0000-0002-5031-3297; etidophysics@gmail.com

Nwachukwu, Iheke Michael – Dr. (Sci.), Department of Physics, Faculty of Science, National Open University of Nigeria, Abuja, Nigeria; https://orcid.org/0000-0003-2237-7805; inwachukwu@noun.edu.ng

Ekechukwu, Christopher Chinasa – Master (Sci.), Department of Physics, Faculty of Physical Science, University of Calabar, Calabar, Nigeria; https://orcid.org/0000-0001-7559-4112; ekehmore@gmail.com

Ekong, Isaac Bassey – Master (Sci.), Department of Physics, Faculty of Physical Science, University of Calabar, Calabar, Nigeria; https://orcid.org/0000-0002-0645-6768; ekongisaac@unical.edu.ng

William, Eddy Sunday – Dr. (Sci.), Department of Physics, School of Pure and Applied Sciences, Federal University of Technology, Ikot Abasi, Nigeria; https://orcid.org/0000-0002-5247-5281; williameddyphysics@gmail.com

Lawal, Kolawole M. – Dr. (Sci.), Professor, Department of Physics, Faculty of Science, National Open University of Nigeria, Abuja Nigeria; kmlawal@noun.edu.ng

Simon, John – Dr. (Sci.), Department of Physics, Faculty of Science, National Open University of Nigeria, Abuja, Nigeria; https://orcid.org/0000-0002-5477-9043; jsimon@noun.edu.ng

Momoh, Kabir O. – Master (Sci.), Department of Physics, Faculty of Science, National Open University of Nigeria, Abuja, Nigeria; https://orcid.org/0009-0006-4512-6397; kmomoh@noun.edu.ng

Oyelami, Oyewole Abiodun – Master (Sci.), Department of Mathematics, Faculty of Science, National Open University of Nigeria, Abuja, Nigeria; https://orcid.org/0000-0002-2599-0595; ooyelami@noun.edu.ng

Appendix A

Some Useful Standard Integrals

$$\int_{r_a}^{r_b} \frac{1}{\sqrt{(r-r_a)(r_b-r)}} dr = \pi_a \tag{A1}$$

$$\int_{r_a}^{r_b} \frac{1}{(a+br)\sqrt{(r-r_a)(r_b-r)}} dr = \frac{\pi_a}{\sqrt{(a+br_b)(a+br_a)}} \tag{A2}$$

$$\int_{r_a}^{r_b} \frac{1}{r}\sqrt{(r-r_a)(r_b-r)} dr = \frac{\pi_a}{2}(r_a+r_b) - \pi_a\sqrt{r_a r_b} \tag{A3}$$

$$\int_{r_a}^{r_b} \frac{1}{r\sqrt{(r-r_a)(r_b-r)}} dr = \frac{\pi_a}{\sqrt{r_a r_b}} \tag{A4}$$